NASA TECHNICAL NOTE

NASA TN D-2860

NASA TN D-2860

GPO PRICE $ _____

CFSTI

~~OTS~~ PRICE(S) $ 2.00

Hard copy (HC) _____

Microfiche (MF) .50

EXTENSION OF AN ANALYSIS OF PERIPHERAL WALL CONDUCTION EFFECTS FOR LAMINAR FORCED CONVECTION IN THIN-WALLED RECTANGULAR CHANNELS

by Joseph M. Savino and Robert Siegel

Lewis Research Center

Cleveland, Ohio

NATIONAL AERONAUTICS AND SPACE ADMINISTRATION • WASHINGTON, D. C. • JUNE 1965

NASA TN D-2860

EXTENSION OF AN ANALYSIS OF PERIPHERAL WALL CONDUCTION EFFECTS FOR LAMINAR FORCED CONVECTION IN THIN-WALLED RECTANGULAR CHANNELS

By Joseph M. Savino and Robert Siegel

Lewis Research Center
Cleveland, Ohio

NATIONAL AERONAUTICS AND SPACE ADMINISTRATION

For sale by the Clearinghouse for Federal Scientific and Technical Information
Springfield, Virginia 22151 – Price $2.00

EXTENSION OF AN ANALYSIS OF PERIPHERAL WALL CONDUCTION EFFECTS FOR LAMINAR FORCED CONVECTION IN THIN-WALLED RECTANGULAR CHANNELS

by Joseph M. Savino and Robert Siegel
Lewis Research Center

SUMMARY

In an earlier analysis the influence of peripheral heat conduction was considered for the condition in which only the broad walls of rectangular ducts were conducting. The heat was generated solely within the broad walls, and the narrow side walls were non-conducting as well as unheated. Both the flow and the heat transfer were assumed to be fully developed.

In this report the previous work has been extended to include two cases of greater generality. The first case was a rectangular duct of arbitrary aspect ratio with uniform heat generation and heat conduction within the broad walls as in the previous analysis. The extension made here is to allow the short walls to also be heat conducting, but with the restriction that a junction of infinite thermal resistance exists between the broad and short sides so that heat flow around the corners cannot occur within the walls.

The temperatures within the duct were governed by a Poisson equation, with the normal derivatives at the boundaries expressed in terms of the second partial derivatives along the boundary to account for the conduction within the walls. An analytical solution was obtained for the temperatures in the fluid and on the boundaries by using a product solution in the form of a Fourier series expansion. The unknown wall temperatures were contained in the integrals required for the Fourier coefficients so that the wall temperatures were expressed by an integral equation. An analytical solution was found, and results were evaluated numerically on a digital computer.

The peripheral conduction within the side walls produced the following effects:

(1) The temperature distribution along the unheated side walls became quite uniform for even small values of wall conductivity.

(2) For aspect ratios less than 5, the temperatures of the heated broad walls were lowered by a significant amount; for aspect ratios greater than 5, only small temperature decreases occurred on the broad walls for a very narrow region adjacent to the corner.

The second case studied was a square duct with uniform heating and peripheral heat conduction in all walls. The solutions provided quantitative information on how the wall temperatures become more uniform as a function of wall conductivity. For large wall conductivity, the results were in agreement with the uniform peripheral wall temperature solution.

INTRODUCTION

In reference 1 an analysis was made of the influence of peripheral wall conduction on the temperature distributions around the perimeter of rectangular channels that were cooled by fully developed laminar forced convection. The channels were heated along part or the entire width of only the broad sides with the short sides left unheated. Wall heat conduction was assumed to take place only within the broad sides; the short sides were of insulating material. Solutions were evaluated for aspect ratios from 1 to ∞ with the wall conductivity varying from 0 to ∞. In the present report the analysis of reference 1 is extended to two more general cases in which all the channel walls are heat conducting. These cases are described as follows.

Case I: The cases considered in reference 1 were models of typical cooling passages employed in flat-plate fuel assemblies of nuclear reactors. In each assembly a series of parallel heat generating plates with coolant flowing between them are supported by unheated side plates. In general, all walls including the side plates are heat conducting with some heat flowing from the fuel plates around the corners into the side plates. Because of the complexity of the most general problem, it was assumed in reference 1 that the side plates were nonconducting. In this report some cases of greater generality are treated that include the side wall conduction. An attempt was made to account for the heat flow around the corner within the walls, but the results for that problem were unsatisfactory because of poor convergence of the Fourier series representing the wall temperature derivatives at the corners. In the present analysis, therefore, it was assumed that no heat flow occurred around the corners within the walls. This assumption eliminated some terms from the more general solution, and the convergence in this case was quite good. The situation with no heat flow around the corner represents a limiting case sometimes encountered in practice where a poor joint exists between the fuel plates and the side support plates, thus providing a high thermal resistance at the corners. Figure 1(a) illustrates this case. The heat generation, which is either supplied

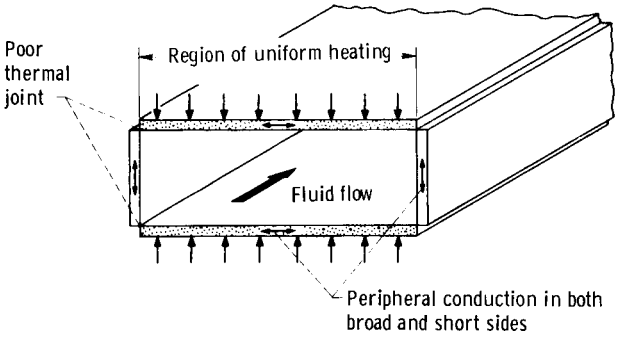

(a) Rectangular channel heated only on broad sides, with peripheral conduction in all sides and no heat flow around corner within the walls.

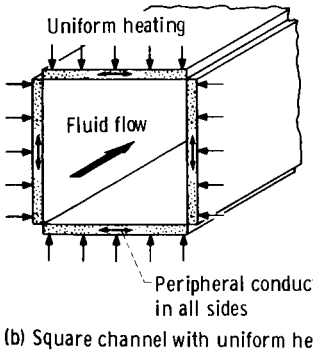

(b) Square channel with uniform heating and peripheral conduction in all sides.

Figure 1. - Models of channels analyzed.

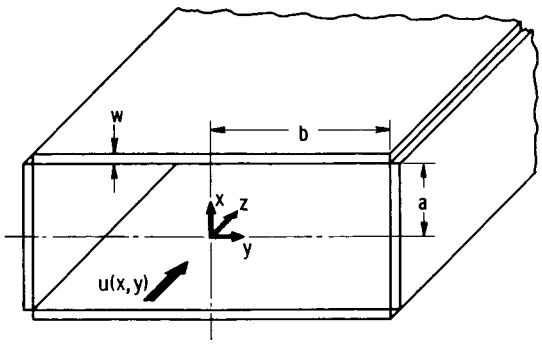

Figure 2. - Coordinate system for model of rectangular thin-wall channel employed in analysis.

to or generated within the walls, is taken to be uniformly supplied over the broad sides. The solution was obtained and the temperature distributions were evaluated for aspect ratios of 1, 2, 5, and 10 for values of the wall conductivity parameter that ranged from 0 to high values.

Case II: The second case considered the effect of peripheral wall conduction on the temperature distribution in a square duct where all four walls conduct heat and are uniformly heated. This geometry is one that is sometimes considered for honeycomb type fuel assemblies in advanced nuclear propulsion devices. The duct configuration is shown in figure 1(b). Temperature distributions were obtained for several wall conductivities between 0 and a high value.

For both cases the fluid motion and the convective heat transfer are assumed to be laminar and fully developed with constant fluid properties. The same type of analytical approach as that in reference 1 is used. An additional part is incorporated into the solution to account for heat being conducted within the two short walls assumed to be insulated in the earlier paper. The additional part leads to a coupling of the temperature distributions for adjacent sides and a simultaneous solution is required.

A similar analysis for turbulent convective heat transfer is not possible because the present state of knowledge of the turbulent mechanism is incomplete, especially for rectangular ducts. The analysis for laminar convection is of value because there are some conditions under which the laminar convection does occur, during reactor shutdown for example. Secondly, the solution for laminar convection will demonstrate in a qualitative way the influence of peripheral conduction on the wall temperatures. The laminar solutions would be expected to provide larger variations of wall temperature around the duct perimeter as compared with the turbulent case.

ANALYSIS

A coordinate system for rectangular (including square) ducts is defined as shown in figure 2. The momentum equation governing the velocity distribution under the conditions of laminar fully developed flow is given by

$$\frac{dp}{dz} = \mu\left(\frac{\partial^2 u}{\partial x^2} + \frac{\partial^2 u}{\partial y^2}\right) \tag{1}$$

(Symbols are defined in appendix A.) When heat is being transferred to the fluid, the temperatures throughout the fluid are determined by the energy equation which, under the assumed fully developed heat-transfer condition, takes the form

$$\rho c_p u \frac{\partial T}{\partial z} = k_f \left(\frac{\partial^2 T}{\partial x^2} + \frac{\partial^2 T}{\partial y^2} + \frac{\partial^2 T}{\partial z^2} \right) \tag{2}$$

where viscous dissipation is assumed negligible. Since the fluid properties ρ, c_p, k_f, and μ are considered to be constant throughout the flow field, the momentum equation (1) and the energy equation (2) are not coupled, and the velocity profile can be determined from equation (1) directly. This has been done and the profile available in Knudsen and Katz (ref. 2, p. 101) is (after rearrangement into a more convenient form)

$$\frac{u}{\bar{u}} = \frac{1 - X^2 + \frac{32}{\pi^3} \sum_{n=1,3,5\ldots}^{\infty} \frac{(-1)^{\frac{n+1}{2}}}{n^3} \left(\frac{e^{-\frac{n\pi\gamma}{2}(1-Y)} + e^{-\frac{n\pi\gamma}{2}(1+Y)}}{1 + e^{-n\pi\gamma}} \right) \cos \frac{n\pi X}{2}}{\frac{2}{3} - \frac{128}{\gamma\pi^5} \sum_{n=1,3,5\ldots}^{\infty} \frac{1}{n^5} \left(\frac{1 - e^{-n\pi\gamma}}{1 + e^{-n\pi\gamma}} \right)} \tag{3}$$

The energy equation can be simplified by making a heat balance for a volume extending over the entire channel cross section and having an incremental length dz. This heat balance results in the following relation:

$$4ab\rho c_p \bar{u} \frac{\partial T_b}{\partial z} = Q$$

where Q is the total heat input per unit channel length and is a constant for all the cases considered here. For fully developed conditions the temperature profiles have the same shape for all z so that

$$\frac{\partial T}{\partial z} = \frac{\partial T_b}{\partial z}$$

Hence,

$$\frac{\partial T}{\partial z} = \frac{Q}{4ab\rho c_p \bar{u}}$$

$$\frac{\partial^2 T}{\partial z^2} = 0$$

Substituting these relations into the energy equation (2) simplifies it to

$$\left.\begin{aligned} \frac{Q}{4ab}\,\frac{u(x,y)}{\bar{u}} &= k_f\left(\frac{\partial^2 T}{\partial x^2} + \frac{\partial^2 T}{\partial y^2}\right) \\ \text{or} \qquad \nabla^2\theta &= \frac{1}{ab}\,\frac{u(x,y)}{\bar{u}} \end{aligned}\right\} \qquad (4)$$

where

$$\theta \equiv \frac{T}{Q/4k_f}$$

Equation (4), Poisson's equation, is to be solved using the velocity profile given by equation (3) and is subject to the particular boundary conditions of interest in this analysis.

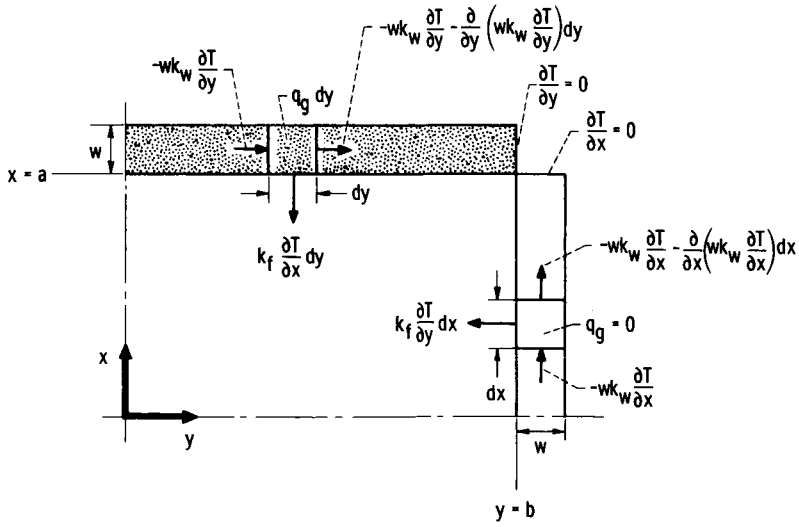

Figure 3. - Terms for heat balances at boundaries with peripheral conduction in walls (for unit axial length of duct).

Case I - Rectangular ducts with uniform internal heating throughout the broad walls only, and with peripheral heat conduction in all walls (no heat conduction around the corner within the walls). - The boundary conditions for this class of problems are derived by performing heat balances on elements of the heated and unheated walls. The terms entering into the heat balances are shown in figure 3 (p. 5). Note that only one quadrant of the duct cross section need be considered because of the symmetry that exists about the coordinate axes. The wall thickness w is considered to be sufficiently thin so that the temperature is constant through the wall thickness and is equal to the local fluid temperature at the wall. The local internal heat generation per unit area q_g will be held constant along the width of the heated wall, although the analytical technique used here can be applied for any prescribed variation of q_g with y. The total heat input per unit channel length in the flow direction Q is related to q_g by the equation $Q = 4bq_g$. Under these restrictions the thermal boundary conditions for the duct quadrant are as follows:

$$x = a, \quad 0 \leq y \leq b \qquad \frac{\partial \theta}{\partial x} = \frac{1}{b} + w \frac{k_w}{k_f} \frac{\partial^2 \theta}{\partial y^2} \tag{5a}$$

$$0 \leq x \leq a, \quad y = b \qquad \frac{\partial \theta}{\partial y} = w \frac{k_w}{k_f} \frac{\partial^2 \theta}{\partial x^2} \tag{5b}$$

$$x = 0, \quad 0 \leq y \leq b \qquad \frac{\partial \theta}{\partial x} = 0 \tag{5c}$$

$$0 \leq x \leq a, \quad y = 0 \qquad \frac{\partial \theta}{\partial y} = 0 \tag{5d}$$

(5c) and (5d): Symmetry conditions

The second derivative terms in (5a) and (5b) account for the peripheral conduction within the walls. When the wall conductivity k_w is 0, the problem reduces to one of uniform heat flux transferred to the fluid from the broad walls of rectangular channels with the short walls nonconducting, a set of conditions that has been treated in references 3 and 4.

One other condition must be specified to complete the mathematical description of the problem. The condition is imposed that no heat be conducted around the corner within the walls at $x = a$, $y = b$, and this is expressed by equating the derivatives along each wall to 0 at the corner. Within the short wall, $y = b$, this condition gives

$$\frac{\partial \theta}{\partial x} = 0 \qquad \text{at} \quad x = a \tag{6a}$$

In the broad wall, x = a, the condition is

$$\frac{\partial \theta}{\partial y} = 0 \qquad \text{at} \quad y = b \tag{6b}$$

An analytical solution will now be obtained for the energy equation (4) subject to boundary conditions (5) and (6).

The solution is derived by applying the method of superposition. As discussed in reference 5 (p. 9), if for a given geometry a solution of Poisson's equation is known for simple boundary conditions, then more complicated boundary conditions can be accounted for by superposing solutions of Laplace's equation. For the present problem the unknown dimensionless temperature θ is replaced by a sum of a Poisson solution and two Laplace solutions:

$$\theta = \theta_{PI} + \theta_{L1} + \theta_{L2} \tag{7}$$

Equation (7) is substituted into the energy equation (4) and the boundary conditions (5) and (6). The resulting relations are divided as follows into three distinct partial differential equations and their boundary conditions:

$$\nabla^2 \theta_{PI} = \frac{1}{ab} \frac{u(x,y)}{\bar{u}} \tag{8a}$$

$$0 \leq x \leq a, \; y = 0, b \qquad \frac{\partial \theta_{PI}}{\partial y} = 0 \tag{8b}$$

$$x = 0, \; 0 \leq y \leq b \qquad \frac{\partial \theta_{PI}}{\partial x} = 0 \tag{8c}$$

$$x = a, \; 0 \leq y \leq b \qquad \frac{\partial \theta_{PI}}{\partial x} = \frac{1}{b} \tag{8d}$$

$$\nabla^2 \theta_{L1} = 0 \tag{9a}$$

$$0 \leq x \leq a, \quad y = 0 \qquad \frac{\partial \theta_{L1}}{\partial y} = 0 \tag{9b}$$

$$0 \leq x \leq a, \quad y = b \qquad \frac{\partial \theta_{L1}}{\partial y} = w \frac{k_w}{k_f} \frac{\partial^2 \theta}{\partial x^2} \tag{9c}$$

$$x = 0, a, \quad 0 \leq y \leq b \qquad \frac{\partial \theta_{L1}}{\partial x} = 0 \tag{9d}$$

$$\nabla^2 \theta_{L2} = 0 \tag{10a}$$

$$0 \leq x \leq a, \quad y = 0, b \qquad \frac{\partial \theta_{L2}}{\partial y} = 0 \tag{10b}$$

$$x = 0, \quad 0 \leq y \leq b \qquad \frac{\partial \theta_{L2}}{\partial x} = 0 \tag{10c}$$

$$x = a, \quad 0 \leq y \leq b \qquad \frac{\partial \theta_{L2}}{\partial x} = w \frac{k_w}{k_f} \frac{\partial^2 \theta}{\partial y^2} \tag{10d}$$

Poisson's equation (8a) and boundary conditions (8b), (8c), and (8d) account for the total heat addition to the channel. This is necessary because a solution to a Laplace problem cannot add or subtract any net amount of heat to or from a closed region. The solution for θ_{L1} adjusts the fluid temperature distribution to account for a redistribution of heat along the short side wall due to the presence of conduction within the wall. The θ_{L2} solution accounts for the conduction along the width of the broad wall. Thus, the original problem has been divided into a forced convection problem with simple boundary conditions and two problems of steady-state conduction.

The solution for θ_{PI} is derived in reference 4, and for convenience the final results are summarized in appendix B. Both $\nabla^2 \theta_{L1} = 0$ and $\nabla^2 \theta_{L2} = 0$ can be satisfied by product solutions of the same general form:

$$\theta_{L1} = \sum_{n=1, 2, 3 \cdots}^{\infty} \overline{B}_n \cos\left(\frac{n\pi x}{a}\right) \cosh\left(\frac{n\pi y}{a}\right) \tag{11}$$

and

$$\theta_{L2} = \sum_{j=1,2,3\cdots}^{\infty} \overline{A}_j \cos\left(\frac{j\pi y}{b}\right)\cosh\left(\frac{j\pi x}{b}\right) \tag{12}$$

where equations (11) and (12) each satisfy their zero normal derivative boundary conditions (9b), (9d), (10b), and (10c). To satisfy the remaining boundary conditions, (9c) and (10d), equations (11) and (12) are each differentiated once (eq. (11) with respect to y and eq. (12) with respect to x), substituted into their respective boundary conditions (9c) and (10d), and then expanded in a Fourier series to give

$$\int_0^a \overline{B}_n\left(\frac{n\pi}{a}\right)\cos^2\left(\frac{n\pi x}{a}\right)\sinh\left(\frac{n\pi b}{a}\right)dx = \int_0^a \left(w\frac{k_w}{k_f}\right)\left.\frac{\partial^2\theta}{\partial x^2}\right|_{y=b} \cos\left(\frac{n\pi x}{a}\right)dx \tag{13}$$

and

$$\int_0^b \overline{A}_j\left(\frac{j\pi}{b}\right)\cos^2\left(\frac{j\pi y}{b}\right)\sinh\left(\frac{j\pi a}{b}\right)dy = \int_0^b \left(w\frac{k_w}{k_f}\right)\left.\frac{\partial^2\theta}{\partial y^2}\right|_{x=a} \cos\left(\frac{j\pi y}{b}\right)dy \tag{14}$$

When each integral on the right side of equations (13) and (14) is integrated twice by parts, and conditions (6a) and (6b) applied in the process, the Fourier coefficients $\overline{A}_j$ and $\overline{B}_n$ are expressed as

$$\overline{B}_n = \frac{-\left(w\frac{k_w}{k_f}\right)\left(\frac{n\pi}{a}\right)^2 \int_0^a \theta(x, b)\cos\left(\frac{n\pi x}{a}\right)dx}{\frac{n\pi}{2}\sinh\left(\frac{n\pi b}{a}\right)} \tag{15}$$

and

$$\overline{A}_j = \frac{-\left(w\frac{k_w}{k_f}\right)\left(\frac{j\pi}{b}\right)^2 \int_0^b \theta(a, y)\cos\left(\frac{j\pi y}{b}\right)dy}{\frac{j\pi}{2}\sinh\left(\frac{j\pi a}{b}\right)} \tag{16}$$

The coefficients in equations (15) and (16) are then substituted into equations (11) and (12), and the resulting expressions are placed in dimensionless form. The hyperbolic functions are converted to exponential form for greater convenience in numerical evaluation, and θ_{L1} and θ_{L2} become

$$\theta_{L1} = \sum_{n=1,2,3\cdots}^{\infty} - 2n\pi K \cos(n\pi X)\left[\frac{e^{-n\pi\gamma(1-Y)} + e^{-n\pi\gamma(1+Y)}}{1 - e^{-2n\pi\gamma}}\right]\left[\int_0^1 \theta(X, 1)\cos(n\pi X)dX\right] \tag{17}$$

$$\theta_{L2} = \sum_{j=1,2,3\cdots}^{\infty} - \frac{2j\pi K}{\gamma} \cos(j\pi Y)\left[\frac{e^{-\frac{j\pi}{\gamma}(1-X)} + e^{-\frac{j\pi}{\gamma}(1+X)}}{1 - e^{-\frac{2j\pi}{\gamma}}}\right]\left[\int_0^1 \theta(1, Y)\cos(j\pi Y)dY\right] \tag{18}$$

The solution for θ is obtained by combining equations (17) and (18) with equation (7):

$$\theta(X, Y) = \theta_{PI}(X, Y) - \sum_{n=1,2,3\cdots}^{\infty} 2n\pi K \cos(n\pi X)\left[\frac{e^{-n\pi\gamma(1-Y)} + e^{-n\pi\gamma(1+Y)}}{1 - e^{-2n\pi\gamma}}\right]\left[\int_0^1 \theta(X, 1)\cos(n\pi X)dX\right]$$

$$- \sum_{j=1,2,3\cdots}^{\infty} \frac{2j\pi K}{\gamma} \cos(j\pi Y)\left[\frac{e^{-\frac{j\pi}{\gamma}(1-X)} + e^{-\frac{j\pi}{\gamma}(1+X)}}{1 - e^{-\frac{2j\pi}{\gamma}}}\right]\left[\int_0^1 \theta(1, Y)\cos(j\pi Y)dY\right] \tag{19}$$

If equation (19) is evaluated at $X = 1$ with Y variable and at $Y = 1$ with X variable, the result is two simultaneous integral equations for the unknown temperature distribution $\theta(1, Y)$ along the heated wall and the temperature distribution $\theta(X, 1)$ along the unheated wall:

$$\theta(1, Y) = \theta_{PI}(1, Y) - \sum_{n=1, 2, 3\cdots}^{\infty} 2n\pi K(-1)^n \left[\frac{e^{-n\pi\gamma(1-Y)} + e^{-n\pi\gamma(1+Y)}}{1 - e^{-2n\pi\gamma}}\right]\left[\int_0^1 \theta(X, 1)\cos(n\pi X)dX\right]$$

$$- \sum_{j=1, 2, 3\cdots}^{\infty} \frac{2j\pi K}{\gamma} \cos(j\pi Y)\left[\frac{1 + e^{-\frac{2j\pi}{\gamma}}}{1 - e^{-\frac{2j\pi}{\gamma}}}\right]\left[\int_0^1 \theta(1, Y)\cos(j\pi Y)dY\right] \qquad (20)$$

$$\theta(X, 1) = \theta_{PI}(X, 1) - \sum_{n=1, 2, 3\cdots}^{\infty} 2n\pi K \cos(n\pi X)\left[\frac{1 + e^{-2n\pi\gamma}}{1 - e^{-2n\pi\gamma}}\right]\left[\int_0^1 \theta(X, 1)\cos(n\pi X)dX\right]$$

$$- \sum_{j=1, 2, 3\cdots}^{\infty} \frac{2j\pi K}{\gamma} (-1)^j \left[\frac{e^{-\frac{j\pi}{\gamma}(1-X)} + e^{-\frac{j\pi}{\gamma}(1+X)}}{1 - e^{-\frac{2j\pi}{\gamma}}}\right]\left[\int_0^1 \theta(1, Y)\cos(j\pi Y)dY\right] \qquad (21)$$

These integral equations can be solved by a method given in reference 6.

The integrals $\int_0^1 \theta(X, 1)\cos(n\pi X)dX$ and $\int_0^1 \theta(1, Y)\cos(j\pi Y)dY$ are constants for each value of the summation indices n and j. These can then be defined as

$$C_n \equiv \int_0^1 \theta(X, 1)\cos(n\pi X)dX \qquad (22)$$

$$D_j \equiv \int_0^1 \theta(1, Y)\cos(j\pi Y)dY \qquad (23)$$

These constants are unknown as they contain the unknown wall temperatures $\theta(X, 1)$ and $\theta(1, Y)$. Equation (20) is now multiplied by $\cos(m\pi Y)dY$ and integrated from Y = 0 to 1:

$$\int_0^1 \theta(1,Y)\cos(m\pi Y)dY = \int_0^1 \theta_{PI}(1,Y)\cos(m\pi Y)dY$$

$$- \sum_{n=1,2,3\cdots}^{\infty} 2n\pi K(-1)^n C_n \int_0^1 \left[\frac{e^{-n\pi\gamma(1-Y)} + e^{-n\pi\gamma(1+Y)}}{1 - e^{-2n\pi\gamma}}\right] \cos(m\pi Y)dY$$

$$- \frac{m\pi K}{\gamma}\left(\frac{1 + e^{-\frac{2m\pi}{\gamma}}}{1 - e^{-\frac{2m\pi}{\gamma}}}\right) D_m \qquad (24)$$

In the evaluation of the last term on the right the following identity was employed:

$$\int_0^1 \cos(j\pi Y)\cos(m\pi Y)dY = \frac{1}{2} \qquad \text{when } j = m$$

$$= 0 \qquad \text{when } j \neq m$$

The term on the left side of equation (24) is equal to D_m. The first term on the right side is defined as

$$E_m \equiv \int_0^1 \theta_{PI}(1,Y)\cos(m\pi Y)dY \qquad (25)$$

The integral in the second term on the right is carried out, and equation (24) can then be written as

$$D_m = E_m - \sum_{n=1,2,3\cdots}^{\infty} 2n\pi K(-1)^n C_n \frac{(-1)^m n\pi\gamma}{(n\pi\gamma)^2 + (m\pi)^2} - \frac{m\pi K}{\gamma}\left(\frac{1 + e^{-\frac{2m\pi}{\gamma}}}{1 - e^{-\frac{2m\pi}{\gamma}}}\right) D_m \qquad (26)$$

Equation (26) is solved for D_m and the result written in the form

$$D_m = e_m + \sum_{n=1,2,3\cdots}^{\infty} f_{mn} C_n \tag{27}$$

where

$$e_m \equiv \frac{E_m}{1 + \left(\frac{m\pi K}{\gamma}\right)\left(\frac{1 + e^{-\frac{2m\pi}{\gamma}}}{1 - e^{-\frac{2m\pi}{\gamma}}}\right)} \tag{28}$$

$$f_{mn} \equiv \frac{-2K(-1)^m(-1)^n}{\gamma\left[1 + \left(\frac{m\pi K}{\gamma}\right)\left(\frac{1 + e^{-\frac{2m\pi}{\gamma}}}{1 - e^{-\frac{2m\pi}{\gamma}}}\right)\right]\left[1 + \left(\frac{m}{n\gamma}\right)^2\right]} \tag{29}$$

In a similar fashion when equation (21) is multiplied by $\cos(\ell\pi X)$ and integrated the following relation is obtained:

$$C_\ell = g_\ell + \sum_{j=1,2,3\cdots}^{\infty} h_{\ell j} D_j \tag{30}$$

where

$$g_\ell \equiv \frac{F_\ell}{1 + \ell\pi K\left[\frac{1 + e^{-2\ell\pi\gamma}}{1 - e^{-2\ell\pi\gamma}}\right]} \tag{31}$$

$$F_\ell \equiv \int_0^1 \theta_{PI}(X, 1)\cos(\ell\pi X)dX \tag{32}$$

$$h_{\ell j} = \frac{-2K(-1)^{\ell}(-1)^{j}}{\left[1 + \ell\pi K\left(\frac{1 + e^{-2\ell\pi\gamma}}{1 - e^{-2\ell\pi\gamma}}\right)\right]\left[1 + \left(\frac{\ell\gamma}{j}\right)^2\right]} \tag{33}$$

Equations (27) and (30) are the sought after simultaneous relations for the unknown integrals C_ℓ and D_m that are contained in the solution for $\theta(X, Y)$ (eq. (19)). If equations (27) and (30) are combined, a single expression is obtained for either the C_ℓ's or D_m's:

$$D_m = \left(e_m + \sum_{n=1, 2, 3\cdots}^{\infty} g_n f_{mn}\right) + \sum_{n=1, 2, 3\cdots}^{\infty} \sum_{\ell=1, 2, 3\cdots}^{\infty} (f_{mn} h_{n\ell}) D_\ell \tag{34}$$

or

$$C_\ell = \left(g_\ell + \sum_{j=1, 2, 3\cdots}^{\infty} e_j h_{\ell j}\right) + \sum_{j=1, 2, 3\cdots}^{\infty} \sum_{n=1, 2, 3\cdots}^{\infty} (h_{\ell j} f_{jn}) C_n \tag{35}$$

Each of these relations is an infinite set of simultaneous equations for either the D_m or C_ℓ. A truncated set of these equations was solved on a digital computer by the technique given by Kantorovich and Krylov (ref. 5, p. 20). Generally about 100 D_m and C_ℓ were required to have the series solution for θ converge. The D_m and C_ℓ decreased at least as well as $1/m^3$ and $1/\ell^3$. The quantities E_m and F_ℓ that appear in the coefficients e_m and g_ℓ were evaluated from the θ_{PI} solution and their analytical forms are given in appendix C. The solution for θ is now complete; however, to be usable in physical problems it must be given relative to the fluid bulk temperature. The dimensionless bulk temperature θ_b is defined as

$$\theta_b = \frac{1}{ab}\int_0^a \int_0^b \frac{u}{\bar{u}}\,\theta\,dx\,dy = \frac{1}{ab}\int_0^a \int_0^b \frac{u}{\bar{u}}\,\theta_{PI}\,dx\,dy$$

$$+ \frac{1}{ab}\int_0^a \int_0^b \frac{u}{\bar{u}}\,\theta_{L1}\,dx\,dy + \frac{1}{ab}\int_0^a \int_0^b \frac{u}{\bar{u}}\,\theta_{L2}\,dx\,dy \equiv \theta_{PI,\,b} + \theta_{L1,\,b} + \theta_{L2,\,b} \tag{36}$$

The $\theta_{PI,b}$ is known from reference 4 and is given in appendix B. Rather than evaluate $\theta_{L1,b}$ and $\theta_{L2,b}$ by direct integration, a much more simple approach is obtained by applying Green's second identity. The procedure will be shown for only the function $\theta_{L1,b}$ as the result for $\theta_{L2,b}$ is found in a similar fashion. The $u/\overline{u}$ in the $\theta_{L1,b}$ integral is eliminated by use of equation (8a), which gives

$$\theta_{L1,b} = \int_0^a \int_0^b \theta_{L1} \nabla^2 \theta_{PI} \, dx \, dy \tag{37}$$

The second form of Green's identity relates the volume and surface integrals for a volume. For the present problem, the velocity and temperature profiles are fully developed and we can choose as a volume a unit length of the duct. Green's identity then provides the following relation composed of a boundary integral (not a line or contour integral) and an area integral over the cross section:

$$\theta_{L1,b} = \int_\Gamma \left(\theta_{L1} \frac{\partial \theta_{PI}}{\partial \nu} - \theta_{PI} \frac{\partial \theta_{L1}}{\partial \nu} \right) ds + \int_0^a \int_0^b \theta_{PI} \nabla^2 \theta_{L1} \, dA \tag{38}$$

where $\partial/\partial\nu$ denotes the normal derivative, ds the elemental length on the boundary, and Γ the boundary. Because $\nabla^2 \theta_{L1} = 0$ (eq. (9a)), the second integral vanishes. The first integral contains normal derivatives of θ_{L1} and θ_{PI} on the region boundaries and these are 0 except at the channel walls. Hence equation (38) takes the form

$$\theta_{L1,b} = \gamma \left. \frac{\partial \theta_{PI}}{\partial X} \right|_{X=1} \int_0^1 \theta_{L1}(1, Y) dY - \frac{1}{\gamma} \int_0^1 \theta_{PI}(X, 1) \left. \frac{\partial \theta_{L1}}{\partial Y} \right|_{Y=1} dX \tag{39}$$

From equation (8d) $\left. \partial\theta_{PI}/\partial X \right|_{X=1} = 1/\gamma$, and the θ_{L1} and $\left. \partial\theta_{L1}/\partial Y \right|_{Y=1}$ are evaluated from equation (17). These quantities are substituted into equation (39) and integrated to give the final result:

$$\theta_{L1,b} = \sum_{n=1,2,3\cdots}^{\infty} 2KC_n \left[(n\pi)^2 F_n - \frac{(-1)^n}{\gamma} \right] \tag{40}$$

Similarly,

$$\theta_{L2,b} = \sum_{j=1,2,3\cdots}^{\infty} \frac{2K}{\gamma} (j\pi)^2 D_j E_j \tag{41}$$

In summary, the final solution for the dimensionless temperature distribution throughout the fluid cross section is given by

$$(\theta - \theta_b) = (\theta_{PI} - \theta_{PI,b}) + (\theta_{L1} - \theta_{L1,b}) + (\theta_{L2} - \theta_{L2,b}) \tag{42}$$

where $(\theta_{PI} - \theta_{PI,b})$ is given in appendix B, θ_{L1} by equation (17), θ_{L2} by equation (18), $\theta_{L1,b}$ by equation (40), $\theta_{L2,b}$ by equation (41), and the integrals D_m and C_j in the Fourier coefficients are found from equations (34) and (35).

Case II - Square duct with uniform internal heating and peripheral heat conduction throughout all the walls. - The analysis for this case will be presented in less detail than that for case I as the basic method is the same. If the dimension 2a is used for the length of the duct side, the relation between the heat generation per unit wall area and the total heat input per unit channel length is

$$Q = 8aq_g$$

The boundary conditions analogous to those in equation (5) then become

$$x = a,\ 0 \leq y \leq a \qquad \frac{\partial\theta}{\partial x} = \frac{1}{2a} + w\frac{k_w}{k_f}\frac{\partial^2\theta}{\partial y^2} \tag{43a}$$

$$0 \leq x \leq a,\ y = a \qquad \frac{\partial\theta}{\partial y} = \frac{1}{2a} + w\frac{k_w}{k_f}\frac{\partial^2\theta}{\partial x^2} \tag{43b}$$

$$x = 0,\ 0 \leq y \leq a \qquad \frac{\partial\theta}{\partial x} = 0 \tag{43c}$$

$$0 \leq x \leq a,\ y = 0 \qquad \frac{\partial\theta}{\partial y} = 0 \tag{43d}$$

From the symmetry of the problem there is no heat flow within the walls around the corner; hence, the derivatives at the corner remain 0 as in equations (6).

The solution is again formed by a superposition of three solutions as in equation (7). The θ_{PII} (the use of II in the subscript distinguishes this solution from θ_{PI} in case I) solution must now account for heat addition along all sides of the duct so that the conditions in equations (8) now become

$$\nabla^2\theta_{PII} = \frac{1}{a^2}\frac{u(x, y)}{\bar{u}} \tag{44a}$$

$$x = a, \quad 0 \leq y \leq a \qquad \frac{\partial\theta_{PII}}{\partial x} = \frac{1}{2a} \tag{44b}$$

$$0 \leq x \leq a, \quad y = a \qquad \frac{\partial\theta_{PII}}{\partial y} = \frac{1}{2a} \tag{44c}$$

$$x = 0, \quad 0 \leq y \leq a \qquad \frac{\partial\theta_{PII}}{\partial x} = 0 \tag{44d}$$

$$0 \leq x \leq a, \quad y = 0 \qquad \frac{\partial\theta_{PII}}{\partial y} = 0 \tag{44e}$$

The conditions for θ_{L1} and θ_{L2} remain the same as in equations (9) and (10) except that the dimension b becomes a for the square configuration.

The solution for θ_{PII} is found from appendix B by letting $\gamma = 1$ and $\beta = 1$, the latter value corresponding to the condition of uniform heating all around the duct boundary.

The solutions for θ_{L1} and θ_{L2} can be obtained from equations (17) and (18) by letting $\gamma = 1$:

$$\theta_{L1} = \sum_{n=1, 2, 3\cdots}^{\infty} -2n\pi K \cos(n\pi X)\left[\frac{e^{-n\pi(1-Y)} + e^{-n\pi(1+Y)}}{1 - e^{-2n\pi}}\right]\left[\int_0^1 \theta(X, 1)\cos(n\pi X)dX\right] \tag{45}$$

$$\theta_{L2} = \sum_{j=1, 2, 3\cdots}^{\infty} -2j\pi K \cos(j\pi Y)\left[\frac{e^{-j\pi(1-X)} + e^{-j\pi(1+X)}}{1 - e^{-2j\pi}}\right]\left[\int_0^1 \theta(1, Y)\cos(j\pi Y)dY\right] \tag{46}$$

Since for a square duct these expressions are symmetric in X and Y,

$$\int_0^1 \theta(X, 1)\cos(n\pi X)dX = \int_0^1 \theta(1, Y)\cos(n\pi Y)dY \equiv S_n \tag{47}$$

When the S_n are found, then θ_{L1} and θ_{L2} will be known and can be added to θ_{PII} to provide the temperature distribution. The S_n are obtained in the same manner as the C_n and D_j in case I. However, since the C_n and D_j would be equal for the present symmetric conditions, equations (27) and (30) simplify to

$$S_m = p_m + \sum_{n=1, 2, 3\cdots}^{\infty} v_{mn}S_n \tag{48}$$

where

$$p_m = \frac{P_m}{1 + (m\pi K)\left(\frac{1 + e^{-2m\pi}}{1 - e^{-2m\pi}}\right)} \tag{49}$$

$$v_{mn} = \frac{-2K(-1)^m(-1)^n}{\left[1 + (m\pi K)\left(\frac{1 + e^{-2m\pi}}{1 - e^{-2m\pi}}\right)\right]\left[1 + \left(\frac{m}{n}\right)^2\right]} \tag{50}$$

and

$$P_m \equiv \int_0^1 \theta_{PII}(X, 1)\cos(m\pi X)dX = \int_0^1 \theta_{PII}(1, Y)\cos(m\pi Y)dY \tag{51}$$

Analytical expressions for P_m are given in appendix C. Equation (48) is an infinite set of simultaneous equations for S_m and was solved as in case I by the methods given in reference 5. Generally about 200 S_m were required to obtain accurate wall temperature distributions.

To be applicable physically the solution has to be related to the bulk temperature θ_b. For the θ_{PII} function the bulk temperature is found from $\theta_{P, b}$ in appendix B by letting $\gamma = 1$ and $\beta = 1$. The values $\theta_{L1, b}$ and $\theta_{L2, b}$, which are equal to each other, are found by following the same procedure leading to equation (40). The only change is

that $\partial\theta_{PII}/\partial X\big|_{X=1}$ is now $1/2$ rather than $1/\gamma$ as used for equation (40) and the notation changes as C_n and F_n are replaced by S_n and P_n, respectively. This yields

$$\theta_{L1,b} = \theta_{L2,b} = \sum_{n=1,2,3\cdots}^{\infty} 2KS_n\left[(n\pi)^2 P_n - \frac{(-1)^n}{2}\right] \tag{52}$$

In summary, the temperature distribution is given by

$$\theta - \theta_b = \left(\theta_{PII} - \theta_{PII,b}\right) + \left(\theta_{L1} - \theta_{L1,b}\right) + \left(\theta_{L2} - \theta_{L2,b}\right) \tag{53}$$

The Poisson solutions θ_{PII} and $\theta_{PII,b}$ are found from appendix B by letting $\gamma = 1$ and $\beta = 1$. The Laplace solutions θ_{L1} and θ_{L2} are given in equations (45) and (46) where the integrals equal to S_n are found from the solution of the simultaneous equations (48). The bulk temperatures $\theta_{L1,b}$ and $\theta_{L2,b}$ are obtained from equation (52).

RESULTS AND DISCUSSION

Case I

The preceding analysis was used to evaluate the dimensionless temperature distributions (1) throughout the fluid cross section for a square duct (figs. 4(a) and (b)) and (2) along the walls for ducts of various aspect ratios (figs. 5(a) to (d)). The isotherms of figures 4(a) and (b) were drawn through temperatures that were calculated from equation (B2) with $\gamma = 1$ and $\beta = 0$ for figure 4(a) and from equation (42) for figure 4(b). In figures 5(a) to (d), for the dimensionless wall temperatures, the origin of the abscissa corresponds to the center of the heated sides. As the curves are followed to the right, the temperature distributions proceed along the heated sides to the corners (from $Y = 0$ to $Y = 1$) and then along the unheated sides from the corners to the center of the unheated sides (from $X = 1$ to $X = 0$). The dimensionless temperatures are governed by two parameters - the channel aspect ratio γ and the parameter K, which is referred to hereafter as the wall to fluid conductivity parameter. Each part of figure 5 is for a different aspect ratio, $\gamma = 1$, 2, 5, and 10. The solutions from the present analysis are given by solid lines, and for each solid curve the corresponding solution of reference 1, where only the heated walls are heat conducting, is given by the dotted lines. The dot-dash lines provide the limiting case when the walls are all nonconducting.

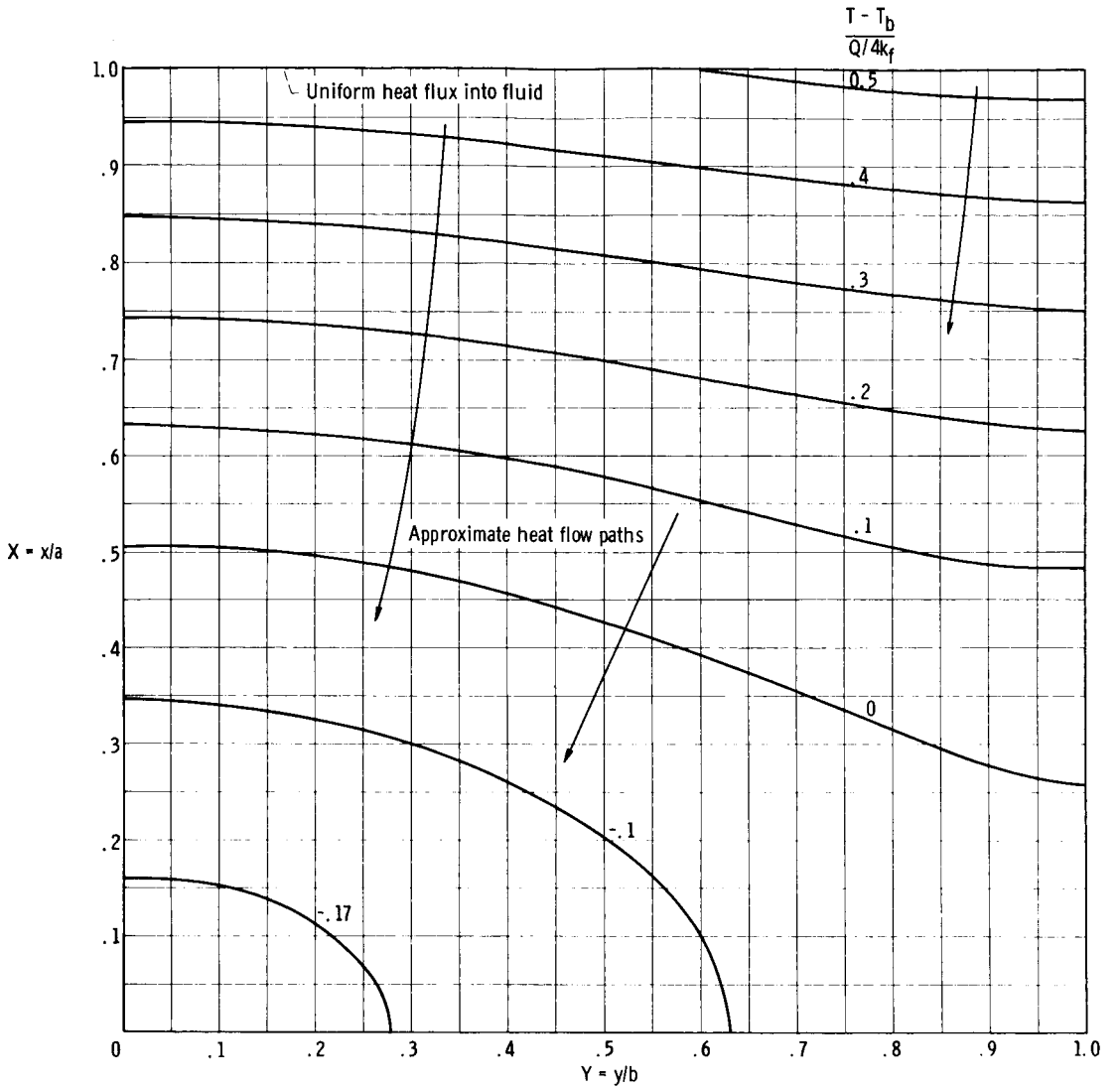

(a) All walls non-heat-conducting, K = 0.

Figure 4. - Isotherms and approximate heat flow directions within fluid for a square duct uniformly heated in two opposite sides only.

An examination and comparison of the isotherms of figure 4, and of the dotted and solid sets of curves in figure 5, clearly reveal the influence of having the unheated walls become heat conducting. Two effects are evident. First, the temperatures along the unheated walls become much more uniform. Secondly, there is a reduction in the temperatures of the heated walls. This reduction is appreciable in channels of small aspect ratio (γ = 1 and 2) and becomes smaller when γ is increased to 5 or 10. To understand this behavior consider that in a square or rectangular duct the convection is poor in the corners because of the low fluid velocities. When only the heated walls are made conducting some of the heat generated near the corner will be conducted peripherally within the walls away from the corners to a region of better convection. This peripheral

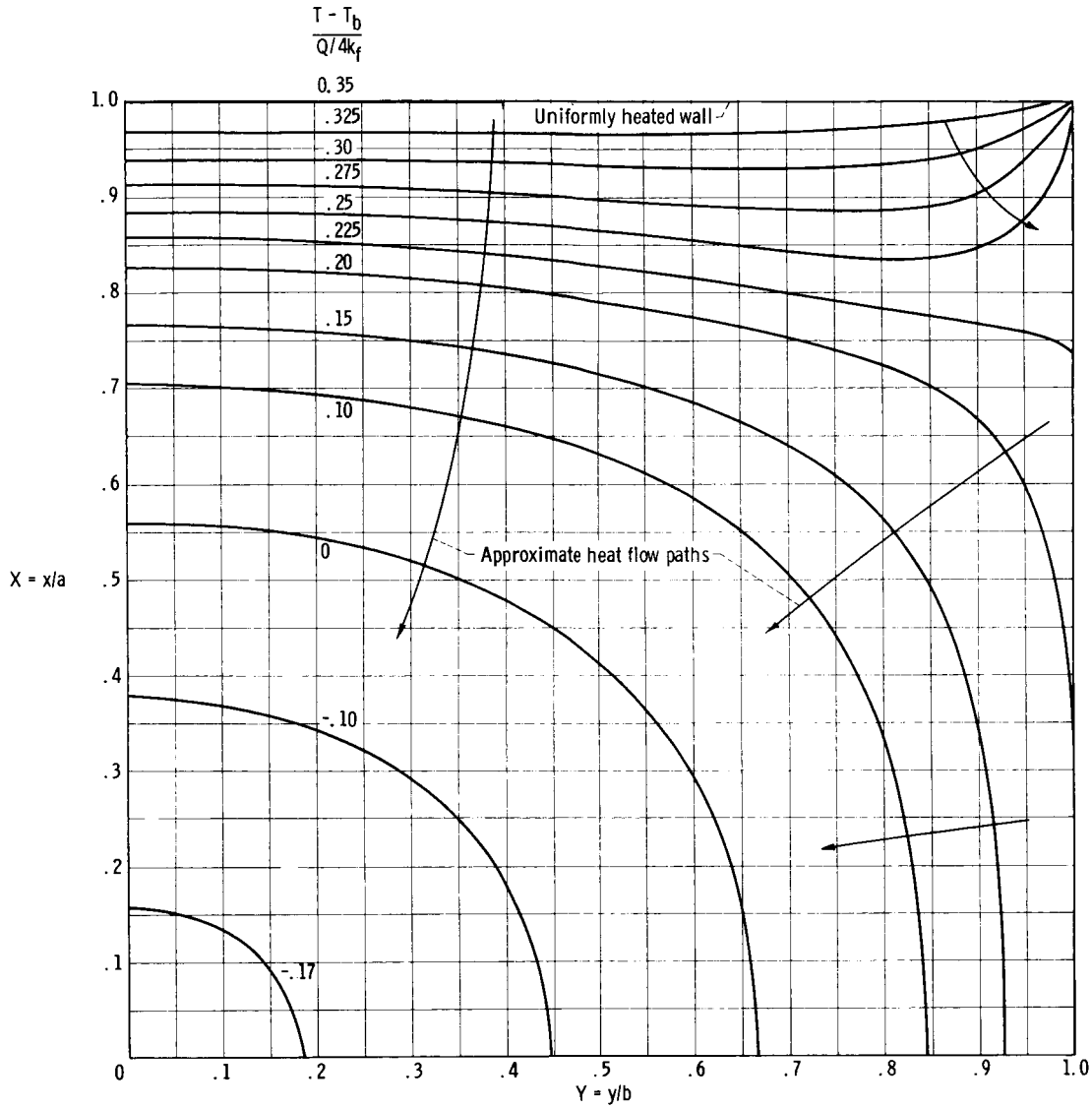

(b) All walls heat conducting, K = 5, with no heat flow around the corners within the walls.

Figure 4. - Concluded.

wall conduction thereby reduces the corner temperatures. Once the heat is redistributed over the conducting walls, it must all be transferred directly from these walls to the fluid. This is indicated in figure 4(a) which, although it is for nonconducting walls (K = 0), is typical of all square ducts with heating and conduction in opposite walls only. This is because conduction in only the two heated walls does not appreciably change the wall temperature distributions as evidenced by the dotted curves in figure 5(a).

When the unheated side walls are also allowed to be heat conducting, these walls provide an additional path for the heat to flow from the heated walls into the fluid. This is seen by examining the patterns of the isothermal lines within the fluid and the resultant heat flow directions for the case when $\gamma = 1$ and K = 5, as shown in figure 4(b). Some

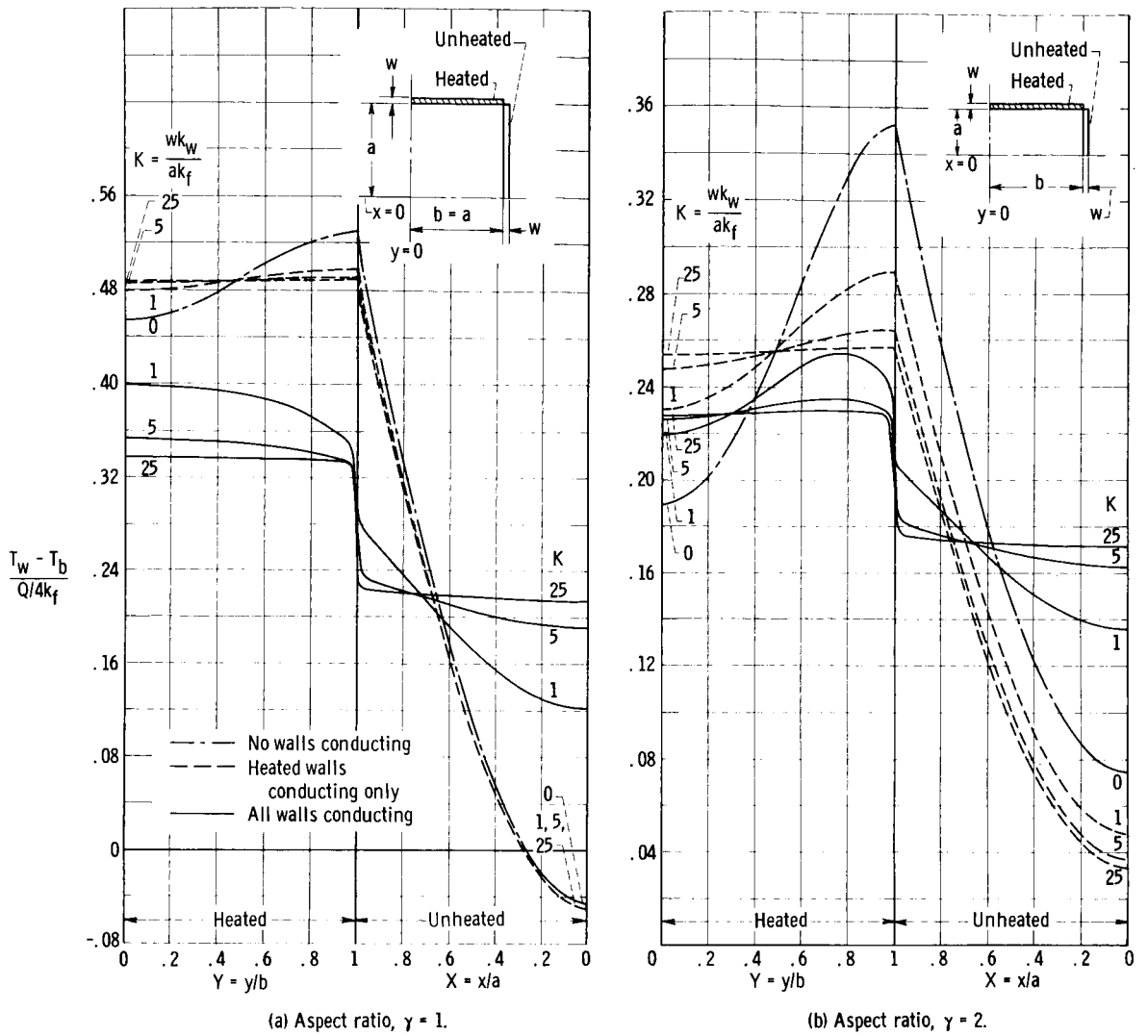

Figure 5. - Wall temperatures with peripheral conduction in (1) no walls, (2) heated walls only, or (3) all walls with no heat flow around corners.

of the heat generated in the heated walls now flows through the fluid in the corner regions to a portion of the unheated walls adjacent to the corners. This heat is then conducted along the unheated walls and is transferred to the fluid in a region of improved convection. Hence, the unheated walls now become somewhat effective as heat-transfer surfaces, and the temperatures along the heated walls are thereby reduced.

One other feature of figure 4(b) is worth noting because it will aid the understanding of the wall temperature curves in figure 5. The heat transfer across the corners causes the isotherms to curve rapidly and group together in the corners. This produces very rapid temperature changes along the walls near the corners and obscures the fact in some cases that the derivatives along the walls are 0 at the corners as imposed on the analysis by equations (6).

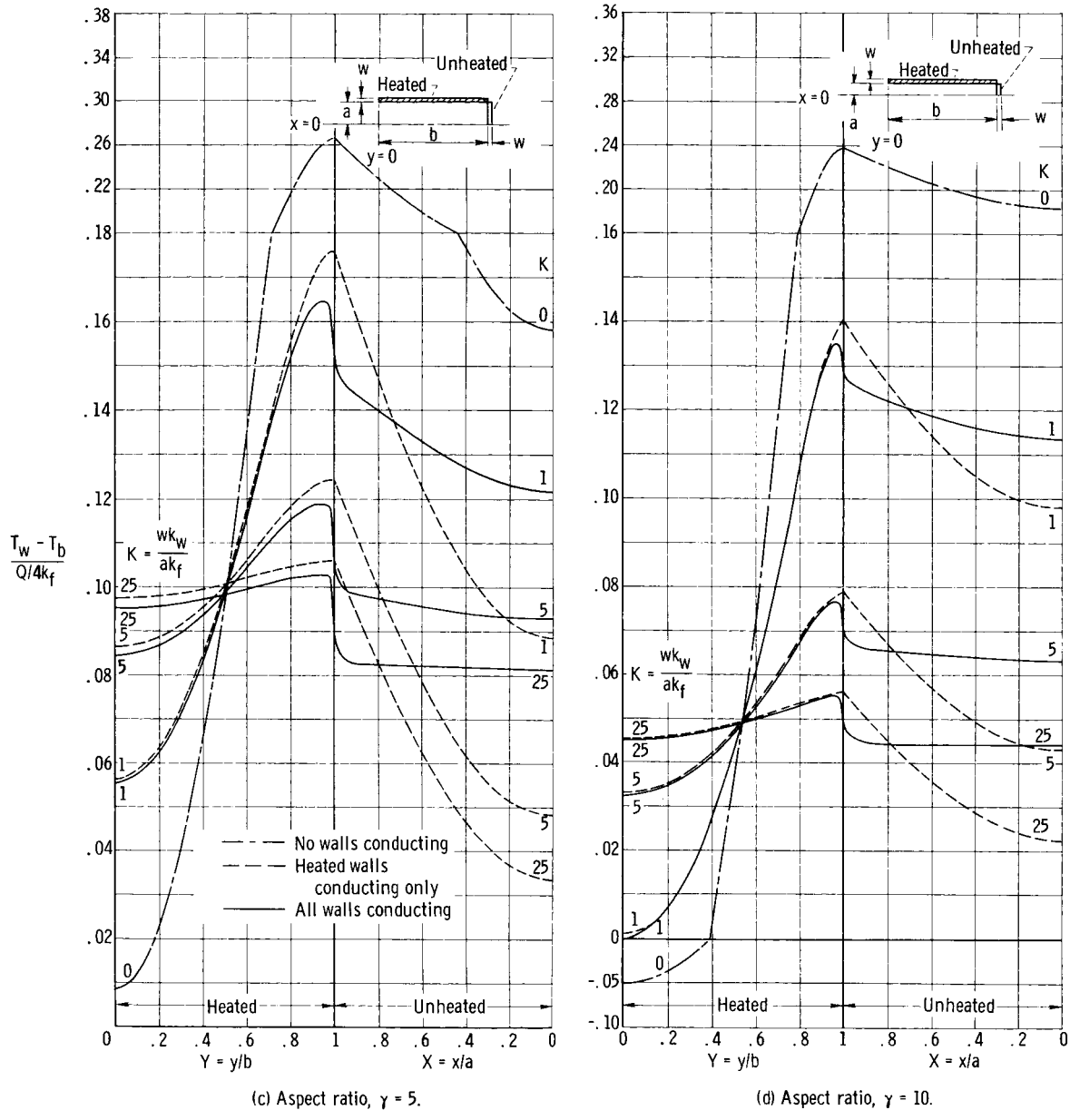

(c) Aspect ratio, γ = 5.

(d) Aspect ratio, γ = 10.

Figure 5. - Concluded

As the aspect ratio is increased, the fact that the short wall occupies less of the total channel perimeter makes the conduction in the short wall proportionately less effective in lowering the temperatures on the heated wall. For an aspect ratio of 10 the conduction in the short unheated walls produces only a small reduction in the temperatures of the heated walls close to the corner.

The effect of increasing the parameter K is also demonstrated in figure 5. As K increases, the temperatures along all walls become more uniform, but have a higher value on the heated walls than on the unheated walls. It is this temperature difference that provides the driving potential for the heat flow from the heated walls, across the

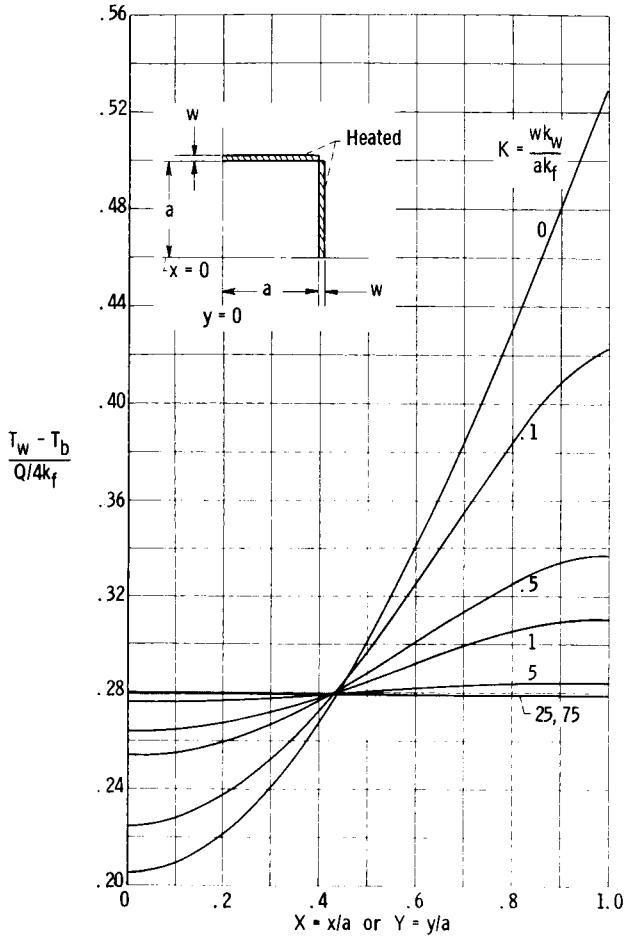

Figure 6. - Wall temperatures of square duct with uniform heating and peripheral conduction in all walls.

fluid in the corner regions to the unheated walls. To obtain an indication of the magnitudes of the K parameter for some physical conditions, a channel is considered where the thickness of the walls is equal to 1/20 the spacing between the broad heated walls, w/2a = 1/20. For aluminum walls with water as a coolant, K is approximately 30. If the wall material is changed to stainless steel, K is reduced to about 3. If the channel is stainless steel and the coolant is a liquid metal, K becomes less than 1.

Case II

The wall temperatures presented here are for a square duct that has uniform heating and peripheral conduction in all walls. Because of symmetry the temperature distributions are the same for all sides; hence, only the distributions extending from the center of one side to the corner need be given. Results are shown in figure 6 for K from 0 to 75. For a small K of unity there is a substantial reduction in the peak temperature and the temperature gradients along the wall. For a K of 25 or greater the temperatures have become uniform and should correspond to the limiting case of a duct having a uniform peripheral temperature with uniform heat addition in the axial direction. As given in reference 3, the Nusselt number for this boundary condition in a square duct is 3.60. When the definitions

$$Nu = \frac{h2a}{k_f}$$

and

$$q_g = \frac{Q}{8a} = h(T_w - T_b)$$

are used, there is obtained

$$\frac{T_w - T_b}{Q/4k_f} = \frac{1}{Nu} = \frac{1}{3.60} = 0.278$$

The value 0.278 is in agreement with the limit for large K in figure 6 and also serves as a check on the correctness of the solutions.

CONCLUSIONS

3 5597

A previous analysis on the effect of peripheral wall heat conduction on the convective heat transfer in rectangular ducts has been extended to study two situations of greater generality and complexity. The peripheral heat conduction within each wall was formulated in terms of an integral equation which was coupled with the energy equation in the fluid. The solutions were obtained in analytical form and evaluated for various aspect ratios and wall conductivities.

Case I: A rectangular duct was considered with uniform heating and peripheral conduction in the broad walls. When the short unheated walls were allowed to conduct heat but no heat was allowed to flow around the corners within the walls, the following changes were found as compared with a duct with nonconducting short walls:

1. For moderate values of the wall conductivity the temperature distribution along the unheated wall became almost uniform.

2. For duct aspect ratios less than 5 the conduction in the unheated wall lowered the dimensionless temperatures along the heated wall. The decrease in the difference between dimensionless wall and bulk temperatures was from 15 to 30 percent depending on the conductivity and aspect ratio. For larger aspect ratios the temperatures along the heated wall were decreased only a small amount for a region near the corner.

Case II: A square duct was considered, heat conducting and uniformly heated on all walls. Moderate values of wall conductivity were found to produce substantial reductions in the peak temperatures that occurred at the duct corners. For high values of the wall conductivity, the duct approached the known case of constant peripheral wall temperature with uniform heat addition in the flow direction.

Lewis Research Center,
National Aeronautics and Space Administration,
Cleveland, Ohio, February 24, 1965.

APPENDIX A

SYMBOLS

A	cross-sectional area
$\overline{A}_j$	Fourier coefficients defined by eq. (16)
A_n	Fourier coefficients defined by eq. (B7)
a	half-length of short side of rectangular duct or half-length of side of square duct
B_n	Fourier coefficients defined by eq. (B9)
$\overline{B}_n$	Fourier coefficients defined by eq. (15)
b	half-length of broad side of rectangular duct
C_n	integral defined by eq. (22)
c_p	specific heat of fluid at constant pressure
D_j	integral defined by eq. (23)
E_m	integral defined by eq. (25)
e_m	coefficient defined by eq. (28)
F_ℓ	integral defined by eq. (32)
f_{mn}	coefficient defined by eq. (29)
G	coefficient defined by eq. (B4)
g_ℓ	coefficient defined by eq. (31)
h	heat-transfer coefficient
$h_{\ell j}$	coefficient defined by eq. (33)
K	wall-to-fluid conduction parameter, wk_w/ak_f
k	thermal conductivity
Nu	Nusselt number
P_m	integral defined by eq. (51)
p	static pressure
p_m	coefficient defined by eq. (49)
Q	total heat-transfer rate to fluid per unit channel length
q_B	heat flux through broad walls
q_g	heat generation rate in wall per unit wall area
q_S	heat flux through short walls
S_n	integral defined by eq. (47)
s	element of surface area around duct perimeter per unit duct length
T	temperature
u	local fluid velocity
$\overline{u}$	integrated mean fluid velocity
v_{mn}	coefficient defined by eq. (50)
w	thickness of channel wall
X	dimensionless coordinate, x/a
x	coordinate measured from center of duct in direction parallel to short sides
Y	dimensionless coordinate, y/b
y	coordinate measured from center of duct in direction parallel to broad sides

z	coordinate measured along channel length
β	ratio of heat fluxes, q_S/q_B
γ	channel aspect ratio, b/a
θ	dimensionless temperature, $4k_fT/Q$
μ	absolute fluid viscosity
ρ	fluid density

Subscripts:

b	integrated bulk mean value
f	fluid
L	Laplace solution
P	Poisson solution
w	wall
I	case I
II	case II
1, 2	distinguishes the two different Laplace solutions

APPENDIX B

SOLUTION FOR θ_{PI} AND θ_{PII}

The solution for Poisson's equation $\theta_P - \theta_{P,b}$ given in reference 4 is for rectangular ducts that are being uniformly heated on each of the four walls, but where the heat flux q_S on the short sides is an arbitrary fraction β, between 0 and 1, of the flux q_B on the broad walls. That is,

$$q_S = \beta q_B \tag{B1}$$

When $\beta = 0$, all the heating is transferred from only the broad walls, and the $\theta_{PI} - \theta_{PI,b}$ solution needed for case I results. When $\beta = 1$, the heat flux is a constant all around the duct periphery. If in addition to $\beta = 1$ the aspect ratio is set equal to 1, the $\theta_{PII} - \theta_{PII,b}$ solution for case II is found.

The general Poisson solution is

$$\theta_P - \theta_{P,b} = \theta_\pi + \theta^* + \theta_1 + \theta_2 - \theta_{P,b} \tag{B2}$$

where each of the θ terms on the right side is given as follows:

$$\theta_\pi(X,Y) = G\left\{\frac{X^4}{96} - \frac{\gamma^2 Y^2}{16} - \frac{8}{\pi^5}\sum_{n=1,2,3\cdots}^{\infty} \frac{(-1)^{\frac{(n+1)}{2}}}{n^5\cosh\left(\frac{n\pi\gamma}{2}\right)}\left[\cosh\left(\frac{n\pi\gamma}{2}Y\right) + \frac{n\pi\gamma}{2}Y\sinh\left(\frac{n\pi\gamma}{2}Y\right)\right]\cos\left(\frac{n\pi X}{2}\right)\right\} \tag{B3}$$

where

$$G = \left[-\frac{\gamma}{12} + \frac{16}{\pi^5}\sum_{m=1,3,5\cdots}^{\infty}\frac{1}{m^5}\tanh\left(\frac{m\pi\gamma}{2}\right)\right]^{-1} \tag{B4}$$

$$\theta^*(X,Y) = \frac{1}{2(\gamma+\beta)}(X^2 - \gamma^2 Y^2) \tag{B5}$$

$$\theta_1(X,Y) = \sum_{n=1,2,3\cdots}^{\infty} A_n \frac{\cosh\left(\frac{n\pi X}{\gamma}\right)}{\sinh\left(\frac{n\pi}{\gamma}\right)} \cos(n\pi Y) \tag{B6}$$

$$A_n = G\left\{\frac{4\gamma^2(-1)^n}{n\pi^6} \sum_{m=1,3,5\cdots}^{\infty} \frac{1}{m^3\left[\left(\frac{m\gamma}{2}\right)^2 + n^2\right]}\left[\frac{m\pi\gamma}{2} + \frac{2n^2}{\left(\frac{m\gamma}{2}\right)^2 + n^2}\tanh\left(\frac{m\pi\gamma}{2}\right)\right]\right\} \tag{B7}$$

$$\theta_2(X,Y) = \sum_{n=1,2,3\cdots}^{\infty} B_n \frac{\cosh(n\pi\gamma Y)}{\sinh(n\pi\gamma)} \cos(n\pi X) \tag{B8}$$

$$B_n = G\left\{\frac{4(-1)^n}{n\pi^6} \sum_{m=1,3,5\cdots}^{\infty} \frac{1}{m^3\left[n^2 - \left(\frac{m}{2}\right)^2\right]}\left[2\tanh\left(\frac{m\pi\gamma}{2}\right) + \left(\frac{m\pi\gamma}{2}\right)\right]\right\} \tag{B9}$$

$$\theta_{P,b} = \frac{\gamma}{\gamma+\beta}\left(\frac{G}{40} + \frac{G\gamma^2}{72}\right) + \frac{G^2\gamma^3}{576} + \frac{131G^2\gamma}{40,320} + \frac{G}{4\pi^3} \sum_{n=1,2,3\cdots}^{\infty} B_n\frac{(-1)^n}{n^3} + \frac{4G^2\gamma}{\pi^8} \sum_{m=1,3,5\cdots}^{\infty} \frac{1}{m^8\cosh^2\left(\frac{m\pi\gamma}{2}\right)}$$

$$+ G \sum_{n=1,3,5\cdots}^{\infty} \tanh\left(\frac{n\pi\gamma}{2}\right)\left\{\frac{1}{(n\pi)^5}\left[\frac{\gamma}{\gamma+\beta}\left(\frac{8}{\gamma} - 8\gamma\right) - G\gamma^2 + \frac{G}{6} - \frac{128}{(\gamma+\beta)(n\pi)^2} - \frac{16G}{(n\pi)^2} + \frac{72G}{(n\pi)^4}\right]\right\}$$

$$+ \frac{G}{\pi^5} \sum_{m=1,3,5\cdots}^{\infty} \sum_{n=1,2,3\cdots}^{\infty} \frac{(-1)^n A_n}{m\left[\left(\frac{m}{2}\right)^2 + \left(\frac{n}{\gamma}\right)^2\right]^2} \frac{\tanh\left(\frac{m\pi\gamma}{2}\right)}{\tanh\left(\frac{n\pi}{\gamma}\right)}$$

$$\times \frac{2G}{\pi^5} \sum_{m=1,3,5\cdots}^{\infty} \sum_{j=1,2,3\cdots}^{\infty} \frac{(-1)^j B_j}{m^2\left[\left(\frac{m}{2}\right)^2 - j^2\right]^2}\left[\frac{m\tanh\left(\frac{m\pi\gamma}{2}\right)}{2\tanh(j\pi\gamma)} - j\right] \tag{B10}$$

APPENDIX C

EXPRESSIONS FOR E_m, F_ℓ, AND P_m

$$E_m = -\frac{(-1)^m}{(m\pi)^2}\left(\frac{G\gamma^2}{8}+\gamma\right)+\frac{A_m}{2}\coth\left(\frac{m\pi}{\gamma}\right)+\sum_{j=1,2,3\cdots}^{\infty}\frac{(-1)^j(-1)^m j\pi\gamma B_j}{(j\pi\gamma)^2+(m\pi)^2} \tag{C1}$$

$$F_\ell = G\left\{\frac{(-1)^\ell\left[(\ell\pi)^2-6\right]}{24(\ell\pi)^4}-\frac{4(-1)^\ell}{\pi^6}\sum_{p=1,3,5\cdots}^{\infty}\frac{1}{p^4\left[\ell^2-\left(\frac{p}{2}\right)^2\right]}\right.$$

$$\left.\times\left[1+\left(\frac{p\pi\gamma}{2}\right)\tanh\left(\frac{p\pi\gamma}{2}\right)\right]\right\}+\frac{(-1)^\ell}{\gamma(\ell\pi)^2}+\frac{B_\ell}{2}\coth(\ell\pi\gamma)+\sum_{r=1,2,3\cdots}^{\infty}(-1)^r A_r\left[\frac{\left(\frac{r\pi}{\gamma}\right)(-1)^\ell}{\left(\frac{r\pi}{\gamma}\right)^2+(\ell\pi)^2}\right] \tag{C2}$$

The coefficient P_m is given by either of the following two forms resulting from the two integrals in equation (51). Although they both give the same numerical results, two different algebraic expressions are found because θ_{PII} has not been used in a symmetric form:

$$P_m = \frac{-(-1)^m}{(m\pi)^2}\left(\frac{G}{8}+\frac{1}{2}\right)+\frac{\coth(m\pi)}{2}(A_m)_{\gamma=1}+\sum_{j=1,2,3\cdots}^{\infty}\frac{(-1)^j(-1)^m j\pi}{(j\pi)^2+(m\pi)^2}B_j\Big|_{\gamma=1} \tag{C3}$$

or

$$P_m = G\left\{\frac{(-1)^m\left[(m\pi)^2 - 6\right]}{24(m\pi)^4} - \frac{4(-1)^m}{\pi^6}\sum_{p=1,3,5\cdots}^{\infty}\frac{1}{p^4\left[m^2 - \left(\frac{p}{2}\right)^2\right]}\left[1 + \frac{p\pi}{2}\tanh\left(\frac{p\pi}{2}\right)\right]\right\}$$

$$+ \frac{(-1)^m}{2(m\pi)^2} + \frac{\coth(m\pi)}{2}\left(B_m\right)_{\gamma=1} + \sum_{r=1,2,3\cdots}^{\infty}\frac{(-1)^r(-1)^m r\pi}{(r\pi)^2 + (m\pi)^2}\left(A_r\right)_{\gamma=1} \qquad \text{(C4)}$$

The Fourier coefficients A_m, $(A_m)_{\gamma=1}$, B_j, and $(B_j)_{\gamma=1}$ are given by equations (B7) and (B9) and G is given by equation (B4).

REFERENCES

1. Siegel, Robert; and Savino, Joseph M.: An Analytical Solution of the Effect of Peripheral Wall Conduction on Laminar Forced Convection in Rectangular Channels. J. Heat Transfer (Trans. ASME), ser. C, vol. 87, no. 1, Feb. 1965, pp. 59-66.

2. Knudsen, J. G.; and Katz, D. L.: Fluid Dynamics and Heat Transfer. McGraw-Hill Book Co., Inc., 1958.

3. Sparrow, E. M.; and Siegel, R.: A Variational Method for Fully Developed Laminar Heat Transfer in Ducts. J. Heat Transfer (Trans. ASME), ser. C, vol. 81, no. 2, May 1959, pp. 157-167.

4. Savino, J. M.; and Siegel, R.: Laminar Forced Convection in Rectangular Channels with Unequal Heat Addition on Adjacent Sides. Int. J. Heat and Mass Transfer, vol. 7, no. 7, July 1964, pp. 733-741.

5. Kantorovich, L. V.; and Krylov, V. I.: Approximate Methods of Higher Analysis. Intersci. Pub., Inc., 1958.

6. Hildebrand, F. B.: Methods of Applied Mathematics. Prentice-Hall Inc., 1952, p. 406.